Does the modulated magnetic structure of $BiFeO_3$ change at low temperatures?

2006 J. Phys.: Condens. Matter 18 2069

(http://iopscience.iop.org/0953-8984/18/6/019)

INSTITUTE OF PHYSICS PUBLISHING JOURNAL OF PHYSICS: CONDENSED MATTER

J. Phys.: Condens. Matter **18** (2006) 2069–2075 doi:10.1088/0953-8984/18/6/019

Does the modulated magnetic structure of $BiFeO_3$ change at low temperatures?

R Przeniosło[1], A Palewicz[1], M Regulski[1], I Sosnowska[1], R M Ibberson[2] and K S Knight[2]

[1] Institute of Experimental Physics, Warsaw University, Hoża 69, PL-00 681 Warsaw, Poland
[2] ISIS Facility, CCLRC—Rutherford Appleton Laboratory, Chilton, Didcot, Oxfordshire OX11 0QX, UK

Received 3 November 2005
Published 27 January 2006
Online at stacks.iop.org/JPhysCM/18/2069

Abstract

High resolution neutron powder diffraction has been applied to verify the model of distorted cycloidal magnetic modulation proposed on the basis of NMR studies of the multiferroic $BiFeO_3$ in Zalesskii *et al* (2000 *Europhys. Lett.* **50** 547). Our experimental results do not support the model of magnetic modulation given by Zalesskii *et al* for $BiFeO_3$ at 4 K. Neutron diffraction patterns recorded at ambient temperature and 4 K agree with the cycloidal magnetic modulation model for $BiFeO_3$ proposed by Sosnowska *et al* (1982 *J. Phys. C: Solid State Phys.* **15** 4835). Present neutron diffraction results are compared with $BiFeO_3$ NMR and Mössbauer literature data.

1. Introduction

Multiferroic materials [1] show a coexistence of electric and magnetic polarizations and have interesting physical properties with potential technical applications. A number of examples of such materials have been found in manganite oxide systems with distorted perovskite structures [2, 3] at low temperatures. This paper is devoted to another transition metal perovskite compound, $BiFeO_3$, in which both ferroelectric and magnetic ordering coexist at room temperature e.g. [4, 5]. The ferroelectric polarization is due to a positional shift of the Fe and Bi ions along the hexagonal $[001]_{hex}$ axis [4]. The magnetic ordering of $BiFeO_3$ at RT proposed in [6] and later confirmed in [7] is a combination of an antiferromagnetic ordering with a cycloidal modulation of period length 620 Å [6]. The modulated magnetic ordering also exists above ambient temperature up to the Néel temperature of $T_N = 640$ K [7]. The presence of the modulated magnetic ordering has a very important physical consequence: the linear magnetoelectric effect disappears in $BiFeO_3$ [8–10]. The modulated magnetic ordering in $BiFeO_3$ has also been confirmed by NMR studies [11–13] and EPR studies [14]. A theoretical description of the modulated magnetic ordering in $BiFeO_3$ has been given in [15].

Several attempts to enhance the magnetoelectric effect in $BiFeO_3$ were achieved by partial replacement of Bi by La [16] and Fe by Mn [17]. It was verified directly by neutron diffraction

that La [18] and Mn [19] doped samples have a longer magnetic modulation length than pure $BiFeO_3$. The enhancement of the dielectric properties observed in Nd [20] and Sm [21] doped $BiFeO_3$ samples as well as in mixed ceramics of $BiFeO_3$–$PbTiO_3$ type [22] is presumably also due to the destruction of the magnetic modulation. It was also shown by EPR studies of bulk $BiFeO_3$ that a magnetic field of 18 T [14] probably destroys the magnetic moment modulation. Further improvements of the magnetoelectric coupling were suggested by studies of $BiFeO_3$ thin films [23, 24].

Recent $BiFeO_3$ low temperature NMR spectrum descriptions given by Zalesskii *et al* [11–13] show that the ordered Fe^{3+} magnetic moment distribution at temperatures below 77 K should be described with a distorted cycloidal modulation (the so called Zalesskii model). The main motivation of the present paper is to obtain experimental evidence that would confirm or negate the Zalesskii model of magnetic modulation in $BiFeO_3$ [11–13].

2. Cycloidal and distorted cycloidal magnetic modulation models

Neutron diffraction is a unique method which gives direct information about the correlations of magnetic moments in the lattice. In the case of collinear ferromagnetic or antiferromagnetic orderings, neutron diffraction contributes to magnetic Bragg peaks [25] at commensurate positions corresponding to the scattering vector $\mathbf{Q}$ equal to reciprocal lattice vectors $\mathbf{G}_{hkl}$:

$$\mathbf{Q} = \mathbf{G}_{hkl} = h \cdot \mathbf{a}^* + k \cdot \mathbf{b}^* + l \cdot \mathbf{c}^* \tag{1}$$

where h, k, l are integer Miller indices and $\mathbf{a}^*$, $\mathbf{b}^*$ and $\mathbf{c}^*$ are the reciprocal lattice vectors. In the case of periodic modulations of the magnetic moments described with one propagation vector $\mathbf{q}$, neutron diffraction contributes to first order magnetic satellite peaks at [25]

$$\mathbf{Q} = \mathbf{G}_{hkl} \pm \mathbf{q}, \tag{2}$$

where the modulation length L is equal to $2\pi/|q|$.

In the case of periodic magnetic moment modulations described with several multiples of the propagation vector $\mathbf{q}$, neutron diffraction contributes not only to first order satellites but also to satellites of higher order like [25]

$$\mathbf{Q} = \mathbf{G}_{hkl} \pm 2\mathbf{q}, \qquad \mathbf{Q} = \mathbf{G}_{hkl} \pm 3\mathbf{q} \qquad \text{etc.} \tag{3}$$

One example of such modulations requiring many propagation vectors is antiphase domains [25]. For neutron diffraction studies of magnetic modulations with long periods the propagation vector length $|q| \ll |G_{hkl}|$, and one needs very high resolution, which is available at backscattering time-of-flight diffractometers, e.g. HRPD at the ISIS facility [26].

The Fe^{3+} ions in $BiFeO_3$ are located on ($6a$) positions of the space group $R3c$ [5]. The magnetic ordering is a combination of a G-type [27] antiferromagnetic ordering subject to a long-range cycloidal modulation. In the model described in [6] (which will be referred to as 'cycloidal') the Fe^{3+} magnetic moments are confined to the plane spanned by the $\mathbf{a} + \mathbf{b}$ and $\mathbf{c}$ axes. The magnetic modulation propagation vector determined from $BiFeO_3$ experimental data [6] is

$$\mathbf{q} = \delta \cdot \mathbf{a}^* + \delta \cdot \mathbf{b}^* \tag{4}$$

where $\delta = 0.0045$. Taking into account the lattice parameters $a = 5.581\,02(4)$ Å and $c = 13.8757(4)$ Å in a hexagonal setting, see e.g. [19], one can calculate that the modulation length $L = 2\pi/|\mathbf{q}| = 620$ Å [6]. In the cycloidal model [6] the Fe^{3+} magnetic moment components are given as a function of ion position $\mathbf{r}$ (please note that M_x, M_y and M_z refer to the crystal axes in the hexagonal setting):

$$\begin{pmatrix} M_x \\ M_y \\ M_z \end{pmatrix} = \begin{pmatrix} M_0 \cos(\mathbf{qr}) \\ M_0 \cos(\mathbf{qr}) \\ M_0 \sin(\mathbf{qr}) \end{pmatrix}. \tag{5}$$

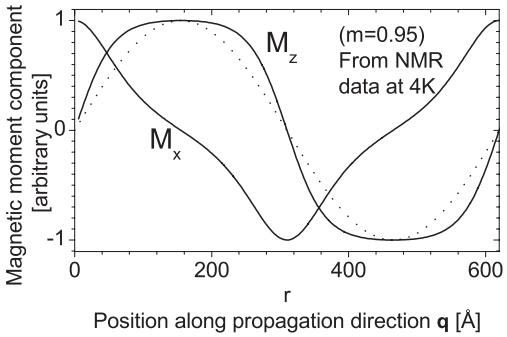

Figure 1. Plot of the ordered Fe^{3+} magnetic moment components $M_x = \mathrm{cn}(A(m)\mathbf{qr}, m)$ and $M_z = \mathrm{sn}(A(m)\mathbf{qr}, m)$ according to the distorted cycloidal model ($m = 0.95$) proposed for $BiFeO_3$ [11–13] at 4 K (solid lines, see equation (6)). These functions are compared with $\sin(\mathbf{qr})$ taken from the cycloidal model (dashed line, see equation (5)). The horizontal axis represents the position r along the modulation propagation direction. All three functions have the same period of 620 Å.

Recent $BiFeO_3$ NMR spectra were interpreted by Zalesskii *et al* [11, 12] by assuming a distorted cycloidal modulated ordering (this model introduced by Zalesskii *et al* will be referred to as 'distorted cycloidal'):

$$\begin{pmatrix} M_x \\ M_y \\ M_z \end{pmatrix} = \begin{pmatrix} M_0\ \mathrm{cn}(A(m)\mathbf{qr}, m) \\ M_0\ \mathrm{cn}(A(m)\mathbf{qr}, m) \\ M_0\ \mathrm{sn}(A(m)\mathbf{qr}, m) \end{pmatrix} \tag{6}$$

where the same propagation vector $\mathbf{q}$ taken from [6] (see equation (4)) is used. The functions $\mathrm{sn}(x, m)$ and $\mathrm{cn}(x, m)$ are the elliptic Jacobi sine and cosine functions while the factor $A(m) = 4K(m)/2\pi$, where $K(m)$ is the complete elliptic integral of the first kind. Both functions on the rhs of equation (6) are periodic with the same modulation length $L = 620$ Å as in the cycloidal model [6]. The ordered total magnetic moment in both cycloidal and distorted cycloidal models is assumed equal M_0 for each Fe^{3+} ion. The functions $\mathrm{sn}(x, m)$ and $\mathrm{cn}(x, m)$ tend to $\sin(x)$ and $\cos(x)$ when $m \to 0$. The parameter m values obtained from NMR data by Zalesskii *et al* [11–13] are $m = 0.48$, 0.83 and 0.95 at 295, 77 and 4.2 K, respectively. That means that the degree of distortion from the sine and cosine functions is largest at low temperature. In order to visualize this effect the functions $\mathrm{sn}(A(m)\mathbf{qr}, m)$ and $\mathrm{cn}(A(m)\mathbf{qr}, m)$ for $m = 0.95$ are shown together with $\sin(\mathbf{qr})$ in figure 1. The Fourier transformation of both $\mathrm{sn}(x, m)$ and $\mathrm{cn}(x, m)$ gives odd order sine and cosine components, respectively.

We have calculated the intensities of the satellite magnetic neutron Bragg peaks located around the (101) and (003) Bragg positions (see e.g [6]) for the cycloidal and distorted cycloidal ($m = 0.95$) magnetic modulation models described above. The resulting neutron powder diffraction patterns of $BiFeO_3$ expected at 4 K for both models are shown in figure 2. The propagation vector is located in the (a, b) plane so the first order satellites associated with $\pm(003)$ contribute to the same peak labelled with $(\delta, \delta, 3)$ in the neutron powder diffraction pattern. The first order satellites associated with $\pm(101)$, $\pm(\bar{1}01)$, $\pm(0\bar{1}1)$ Bragg positions [6] contribute to three resolved peaks which are labelled as 'L', 'R' and 'C' for left, right and central, respectively. The first order satellites' intensity ratios in the cycloidal and distorted cycloidal models are different because of the different values of the first order Fourier terms for the M_z and M_x components (see the function plots in figure 1). The distorted cycloidal model ($m = 0.95$) also contributes to third order satellites, which are denoted with arrows and labelled with 'L3q' and 'R3q' for the left and right, respectively. The fifth and higher order satellites exist but they are too weak to be considered.

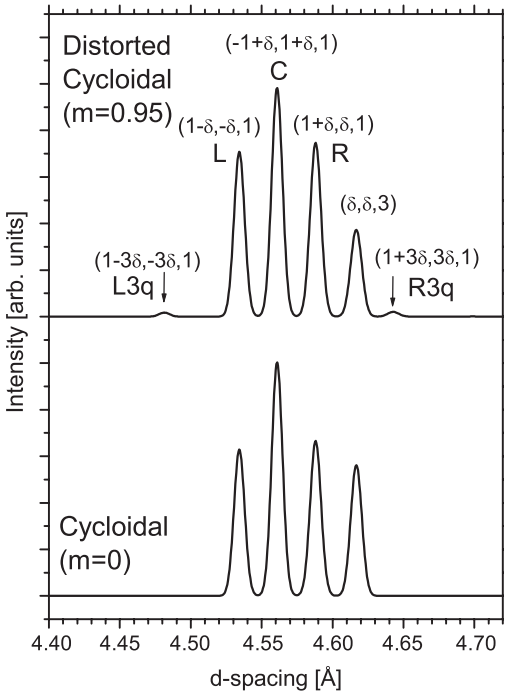

Figure 2. Simulated neutron powder diffraction patterns showing the magnetic satellite peaks expected for $BiFeO_3$ at 4 K. The patterns contain magnetic satellite Bragg peaks associated with the $\pm(101)$, $\pm(\bar{1}01)$, $\pm(0\bar{1}1)$ and $\pm(003)$ reciprocal lattice points. The calculated patterns for the distorted cycloidal ($m = 0.95$) and cycloidal modulation models are shown on the upper and lower panels, respectively. The satellite peaks in both models have the same positions. The labelling in the upper panel shows the Miller indices together with the symbols 'L', 'R', 'C', 'L3q' and 'R3q' used further in the text.

3. Experimental details

Neutron powder diffraction measurements of $BiFeO_3$ have been performed at the high resolution time-of-flight (TOF) neutron diffractometer HRPD at the ISIS facility [26]. The polycrystalline powder $BiFeO_3$ sample was placed in a cylindrical vanadium container of 11 mm diameter inside a helium-flow cryostat. Data were recorded at ambient temperature and 4 K over an interplanar d-spacing range of 3.8–4.8 Å, i.e. in the region with the most intense magnetic satellites around (101) and (003) and one nuclear Bragg peak (012). The measured neutron diffraction intensities have been normalized to the incident beam monitor profile and corrected for detector efficiency effects using previously recorded vanadium calibration data. Sections of the $BiFeO_3$ diffraction patterns obtained at RT and 4 K are shown in figure 3 with the same labelling as in figure 2.

4. Results

Both patterns recorded at RT and 4 K show a similar set of magnetic satellite peaks which correspond to modulation lengths of 632(20) and 637(20) Å at 4 K and RT, respectively. The difference in the peak positions is due to the thermal expansion of the lattice. The heights of the measured magnetic Bragg peaks differ from these calculated (see figure 2) because of

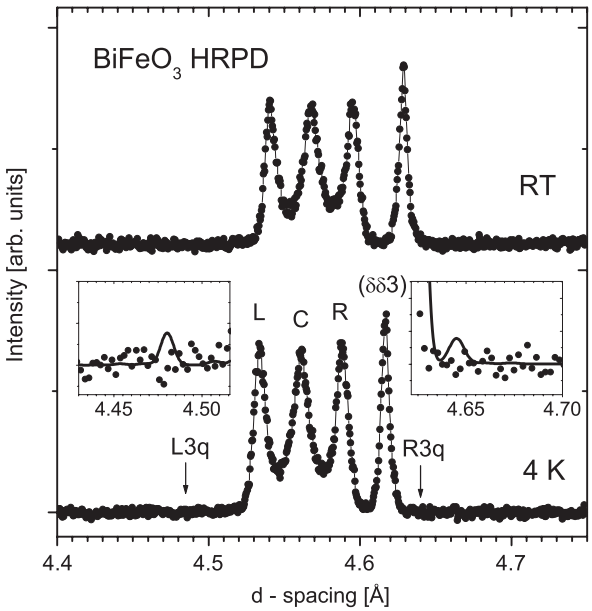

Figure 3. Neutron powder diffraction patterns of $BiFeO_3$ with magnetic satellite peaks measured on HRPD at ambient temperature (upper) and 4 K (lower). The positions of the third order satellites expected for the distorted cycloidal modulation model at 4 K are labelled with 'L3q' and 'R3q'. The inset shows the enlarged part of the 4 K pattern (solid dots) with the profiles of the expected third order satellites calculated assuming the distorted cycloidal model with $m = 0.95$ (solid line).

considerable differences of the peak widths observed in the same pattern. The widths of the nuclear Bragg peak (012) (not shown in figure 3) and the magnetic satellite peak (003) both correspond to $\Delta d/d = 1.50 \times 10^{-3}$ which is close to the instrumental resolution of HRPD in the experimental configuration used. On the other hand, the three magnetic satellite peaks 'L', 'C' and 'R' are much broader with $\Delta d/d = 2.2 \times 10^{-3}, 4.0 \times 10^{-3}$ and 2.2×10^{-3}, respectively. This result has been observed previously in neutron diffraction studies of $BiFeO_3$ at RT and explained in [6] by assuming the cycloidal model with a Gaussian distribution of the propagation vector **q** directions around the [110] direction in the (a, b) plane. In this paper we conclude that this effect occurs not only at ambient temperature but also at 4 K.

In order to compare our diffraction patterns with earlier results [6] and model calculations the following intensity ratios are calculated.

$$A = \frac{I_{\delta\delta 3}}{I_{\mathrm{L}} + I_{\mathrm{R}} + I_{\mathrm{C}}} \tag{7}$$

$$B = \frac{I_{\mathrm{C}}}{I_{\mathrm{L}} + I_{\mathrm{R}}} \tag{8}$$

$$C = \frac{I_{\mathrm{L}3q} + I_{\mathrm{R}3q}}{2I_{\mathrm{C}}} \tag{9}$$

where I_{X} corresponds to the intensity of the peaks labelled with 'X' as shown in figure 3. The values of these ratios determined in the experiment and calculated for the cycloidal and distorted cycloidal models at RT and 4 K are compared in table 1. The present (see figure 3) and past [6, 7] results obtained at RT are in good agreement with each other and they also agree with the cycloidal model calculations. It should also be noted that the experimental results obtained at RT differ little from the distorted cycloidal model ($m = 0.48$) results; the third

Table 1. Values of the magnetic satellites' intensity ratios A, B and C as explained in the text. 'Cycloidal' and 'Dist. cycloidal' refers to model calculations while 'Measured' refers to present neutron diffraction measurement results. The distorted cycloidal model calculations were done by assuming $m = 0.48$ at RT [12] and $m = 0.95$ at 4 K [13]. Previous measurements [6] at ambient temperature gave $A = 0.236(6)$ and $B = 0.79(8)$.

	Cycloidal RT	Dist. cycloidal RT ($m = 0.48$)	Measured RT	Cycloidal 4 K	Dist. cycloidal 4 K ($m = 0.95$)	Measured 4 K
A	0.244	0.220	0.235(11)	0.243	0.147	0.223(9)
B	0.773	0.742	0.800(40)	0.773	0.653	0.778(30)
C	—	0.001	<0.01	—	0.018	<0.01

order satellites calculated for this model ($m = 0.48$) are too weak to be observed in the present and past [6] measurements at RT.

At 4 K the observed intensity ratios agree with the cycloidal and disagree with the distorted cycloidal ($m = 0.95$) model calculations. The intensity ratios A and B differ by about 35% and 15% respectively, i.e. far outside statistical error. The third order satellites predicted by the distorted cycloidal model at 4 K ($m = 0.95$) were not observed in the experimental data as shown in the inset of figure 3.

5. Conclusions

The most important conclusion of the present study is that the magnetic ground state ordering in $BiFeO_3$ does not change much on cooling from RT down to 4 K. Combining this with earlier high temperature $BiFeO_3$ neutron diffraction studies [7] we can conclude that the character of the modulated cycloidal ordering of the Fe^{3+} magnetic moments remains the same from 4 K up to the Néel temperature of 640 K. The only detectable changes of the magnetic satellite Bragg peaks are due to the variation of the ordered magnetic moment and the thermal lattice expansion. The magnetic modulation length remains unchanged within statistical errors. Our data cannot support the distorted cycloidal model of the modulated magnetic ordering proposed by Kozheev *et al* [13] at 4 K. The lack of changes of the modulated magnetic ordering character in $BiFeO_3$ at all temperatures shows that the magnetic interactions in this material are remarkably stable. $BiFeO_3$ is unique among other ferrite systems with distorted perovskite structure, e.g. rare earth orthoferrites $RFeO_3$, in which the magnetic ordering often changes with temperature [28–30].

The present disagreement between $BiFeO_3$ neutron diffraction and NMR studies should be discussed and compared with $BiFeO_3$ Mössbauer studies. NMR [11–13] and Mössbauer studies [31] show two main values of hyperfine fields at the Fe sites in $BiFeO_3$; the larger and smaller fields are labelled as $H_\parallel$ and $H_\perp$, respectively. The value of these hyperfine fields normalized to their low temperature value, i.e. $H_\parallel(T)/H_\parallel(0)$ and $H_\perp(T)/H_\perp(0)$, show the same temperature dependence both in NMR [12, 13] and Mössbauer [31] measurements. On the other hand, these hyperfine fields also agree with the normalized ordered magnetic moment $M(T)/M(0)$ determined from $BiFeO_3$ moderate resolution neutron diffraction studies [32]. There are however two important discrepancies between NMR and Mössbauer results.

First, the relative difference between $H_\parallel$ and $H_\perp$ given by NMR [11–13] is about 1.1%, while Mössbauer studies show 0.5%–0.6% [31].

Second, the NMR spectra become increasingly asymmetric as temperature decreases [11–13], while Mössbauer spectra do not show this effect. $BiFeO_3$ Mössbauer spectra

observed at 412 and 80 K [31] do not show visible asymmetry and they can be described with the same values of the electric field gradient (ΔE_Q) and isomer shift (IS) [31].

The present results clearly demonstrate the need for a more realistic model of the spatial distribution of the magnetic moments and internal fields acting on Fe^{3+} ions in $BiFeO_3$ that would agree with NMR, Mössbauer and neutron diffraction studies in this material.

Acknowledgments

This work (RP, IS) was supported by the Ministry of Science and Education (Poland) and the European Commission through contract no RII3-CT-2003-505925.

References

[1] Hill N A 2000 *J. Phys. Chem.* B **104** 6694
[2] Lottermoser T, Lonkai T, Amann U, Hohlwein D, Ihringer J and Fiebig M 2004 *Nature* **430** 541
[3] Kimura T, Goto T, Shintani H, Ishizaka K, Arima T and Tokura Y 2003 *Nature* **426** 55
[4] Teague J R, Gerson R and James W J 1970 *Solid State Commun.* **8** 1073
[5] Michel C, Moreau J M, Achenbach G D, Gerson R and James W J 1969 *Solid State Commun.* **7** 701
[6] Sosnowska I, Peterlin-Neumaier T and Steichele E 1982 *J. Phys. C: Solid State Phys.* **15** 4835
[7] Sosnowska I, Loewenhaupt M, David W I F and Ibberson R M 1992 *Physica* B **180/181** 117
[8] Tabares-Muñoz C, Rivera J P, Bezinge A, Schmid H and Monnier A 1985 *Japan. J. Appl. Phys.* **24** 1051
[9] Kubel F and Schmid H 1990 *Acta Crystallogr.* B **46** 698
[10] Kadomtseva A M, Zvezdin A K, Popov Y F, Pyatyakov A P and Vorobiev G P 2004 *JETP Lett.* **79** 571
[11] Zalessky A V, Frolov A A, Khimich T A, Bush A A, Pokatilov V S and Zvezdin A K 2000 *Europhys. Lett.* **50** 547
[12] Zalesskii A V, Zvezdin A K, Frolov A A and Bush A A 2000 *JETP Lett.* **71** 465
[13] Kozheev D F, Zalessky A V, Gippius A A, Morozova E N and Bush A A 2003 *Physica* B **329–333** 848
[14] Ruette B, Zvyagin S, Pyatakov A, Bush A, Li J F, Belotelov V, Zvezdin A and Viehland D 2004 *Phys. Rev.* B **69** 064114
[15] Sosnowska I and Zvezdin A K 1995 *J. Magn. Magn. Mater.* **140/141** 167
[16] Murashov A, Rakov D N, Dubienko I S, Zvezdin A K and Ionov V M 1991 *Sov. Phys.—Crystallogr.* **35** 538
[17] Yang C H, Koo T Y and Jeong Y H 2005 *Solid State Commun.* **134** 299
[18] Sosnowska I, Loewenhaupt M, David W I F and Ibberson R M 1993 *Mater. Sci. Forum* **133–136** 683
[19] Sosnowska I, Schäfer W, Kockelmann W, Andersen K H and Troyanchuk I O 2002 *Appl. Phys.* A **74** S1040
[20] Mathe V L, Patankar K K, Patil R N and Lohkande C D 2004 *J. Magn. Magn. Mater.* **270** 380
[21] Mathe V L 2003 *J. Magn. Magn. Mater.* **263** 344
[22] Wang N, Cheng J, Pyatakov A, Zvezdin A K, Li J F, Cross L E and Viehland D 2005 *Phys. Rev.* B **72** 104434
[23] Wang J *et al* 2003 *Science* **299** 1719
[24] Bai F, Wang J, Wuttig M, Li J, Wang N, Pyatakov A P, Zvezdin A K, Cross L E and Viehland D 2005 *Appl. Phys. Lett.* **86** 032511
[25] Bacon G E 1975 *Neutron Diffraction* (Oxford: Clarendon) p 266
[26] Ibberson R M, David W I F and Knight K S 1992 *Rutherford Appleton Lab. Report* RAL-92-031
[27] Bertaut E F 1962 *Magnetism III* ed G T Rado and H Suhl (New York: Academic) p 149
[28] Landolt-Börnstein 1994 *Numerical Data and Functional Relationships in Science and Technology* vol III/27f ed H P J Wijn (Berlin: Springer)
[29] Yamaguchi T 1974 *J. Phys. Chem. Solids* **35** 479
[30] Sławiński W, Przeniosło R, Sosnowska I and Suard E 2005 *J. Phys.: Condens. Matter* **17** 4605
[31] Blaauw C and van der Woude F 1973 *J. Phys. C: Solid State Phys.* **6** 1422
[32] Fischer P, Połomska M, Sosnowska I and Szymański M 1980 *J. Phys. C: Solid State Phys.* **13** 1931